

through mail or telephone interviews, whether they had been told by a physician that their child had AD. Information on lifestyle factors and other potential risk factors, including breastfeeding history (exclusive breastfeeding, partial breastfeeding, or milk formula feeding), also was collected with a parental questionnaire.

Skin Physiologic Measurements

Stratum corneum hydration was measured on the forehead, cheek, flexor aspect of the forearm near the cubital fossa, and chest at 5 to 10 hours after delivery and then once daily until 5 days after delivery. All tests were performed in open cribs in a controlled environment, with room temperature ranging from 22°C to 24°C and humidity at 50%. Skin temperature remained stable during the examination for all newborns. Stratum corneum hydration was measured by using a moisture meter (ASA-M1; Asahi Biomed, Tokyo, Japan),¹⁰ based on capacitance and electrical conductance determined at 2 different frequencies (160 Hz and 143 kHz) with 2 concentric surface electrodes. The probe was pressed on the skin surface for 1 to 2 seconds. Each measurement was obtained twice at the same site; data were rejected when children were crying or visibly sweating. Parameters obtained were moisture content on the skin surface and moisture content in the stratum corneum.

Multiplex Cytokine Array Analysis

Multiplex cytokine array analysis was performed by using the Bio-Plex protein array system (Bio-Rad Laboratories, Hercules, CA), using Luminex-based technology.¹¹ With this assay, we quantitated cytokines simultaneously in serum from cord blood, including IL-1 β , IL-2, IL-4, IL-5, IL-6, IL-7, IL-8, IL-10, IL-12, IL-13, and IL-17, IFN- γ , and TNF- α , granulocyte/macrophage colony-stimulating factor, granulocyte colony-stimulating factor, monocyte chemoattractant protein (MCP)-1, and macrophage inflammatory protein (MIP)-1 β . Most standard curves ranged between 0.2 pg/mL and 3200 pg/mL. At higher and lower concen-

trations, standard curves became flat and lost linearity. Lower limits of detection for the assays used were 0.2 pg/mL for all cytokines studied. Samples with undetectable concentrations were assigned a value of 0.1 pg/mL (ie, halfway between 0 and the lower limit of detection for the assay).

Statistical Methods

The relationship between eczema in infancy and various maternal and perinatal risk factors was assessed by using Pearson χ^2 tests. Differences in clinical characteristics at birth and in skin physiologic parameters between children with and without AD in the first year of life were analyzed by using Student's *t* tests. Because the distribution of cytokines is highly skewed, with many values below the lower limit of detection, the Mann-Whitney *U* test was used to compare cytokine concentrations in cord blood between children with and without AD or infantile eczema. Multivariate logistic regression models were used to determine independent effects of different factors associated with AD in this population; results are expressed as odds ratios (ORs) with 95% confidence intervals (CIs). Subject characteristics and prenatal factors that were statistically significant in Pearson χ^2 tests, Student's *t* tests, or Mann-Whitney *U* tests were included in the multivariate model.

RESULTS

Family History and Prenatal Factors

Children in this study were monitored prospectively, and questionnaire data from 213 (79%) were collected to assess the incidence of AD during the first year of life. The cumulative incidence of maternally reported, physician-diagnosed AD in the cohort was 27 cases (12.4%) among 213 children. Infant gender, method of delivery, length of gestation, birth weight, and maternal age did not differ between children with and without AD (Table 1). Exclusive breastfeeding was not related to the devel-

Perinatal and Postnatal Characteristics of Infants With AD or Infantile Eczema

	AD			Infantile Eczema		
	Yes (N = 27)	No (N = 186)	P	Yes (N = 26)	No (N = 187)	P
Male/female, n	16/11	85/100	.706	17/9	85/102	.057
Cesarean section, n (%)	3 (11.1)	26 (14.0)	.916	5 (19.2)	121 (11.2)	.396
Gestational age, mean \pm SD, wk	40.1 \pm 1.2	39.9 \pm 1.1	.343	39.8 \pm 1.1	39.9 \pm 1.1	.692
Birth weight, mean \pm SD, g	3068 \pm 310	3121 \pm 337	.462	3119 \pm 299	3114 \pm 339	.935
Maternal age, mean \pm SD, y	27.7 \pm 3.0	28.2 \pm 4.3	.534	27.7 \pm 3.8	28.2 \pm 4.2	.551
Breastfeeding, n (%)	14 (51.9)	102 (54.8)	.771	13 (50)	103 (55.1)	.626
Infantile eczema, n (%)	6 (22.2)	20 (10.8)	.089			
Maternal infection, n (%)						
Bacterial ^a	5 (18.5)	22 (11.8)	.135	2 (7.7)	22 (11.8)	.549
Viral ^b	11 (40.7)	81 (43.5)	.783	15 (57.7)	77 (41.2)	.111

^a Urinary tract infection or vaginal infection with *Chlamydia* spp, *Escherichia coli*, group B streptococci, or other bacteria.

^b Upper airway infection or viral gastroenteritis.

opment of AD (Table 1). Rates of maternal bacterial or viral infection during pregnancy did not differ between the 2 groups (Table 1). The diagnosis was >3 times as likely among infants born to mothers with a history of eczema, compared with those born to mothers with no such history. Paternal history of eczema did not influence the likelihood of AD, whereas paternal history of hay fever was associated with less occurrence of AD (Table 2).

The incidence of physician-diagnosed infantile eczema at the age of 1 month was 26 cases (12.1%) among 213 children (Tables 1 and 2). Infantile eczema was more common in male infants than in female infants, although this gender difference was not significant. Infants with infantile eczema were likely to develop AD during the first year (Table 1). Parental history of atopy was not related to the likelihood of infantile eczema (Table 2).

Cytokine Profiles

The proportions of samples with detectable cytokine concentrations were 22% for IL-2, 1% for IL-4, 87% for IL-6, 99% for IL-8, 46% for IL-10, 43% for granulocyte/macrophage colony-stimulating factor, 31% for IFN- γ , 55% for TNF- α , 52% for IL-1 β , 36% for IL-5, 91% for IL-7, 16% for IL-12, 30% for IL-13, 48% for IL-17, 70% for granulocyte colony-stimulating factor, 100% for MCP-1, and 100% for MIP-1 β . No additional analyses of IL-4 were performed, because of the small number of samples with detectable concentrations. Associations between cord blood cytokines and AD outcomes were analyzed first as a categorical variable (detectable or undetectable) and then in terms of concentrations. There was no difference in the categorical variable for each cytokine between children with and without AD (data not shown). Table 3 compares cytokine concentration profiles in cord blood samples from infants with or without development of AD during their first year. MIP-1 β levels were significantly lower in samples from infants who developed AD than in those from infants who did not. A trend toward decreased IL-7 and MCP-1 concentrations in infants with AD fell short of significance (Table 3).

Unlike AD, infants who developed infantile eczema had significantly higher cord blood concentrations of IL-5, IL-17, and MCP-1 than did those who did not (Table 3).

Skin Parameters

The moisture content of the skin surface and that in the stratum corneum were significantly lower on the forehead, cheek, chest, and forearm on postnatal days 2 to 4 than at the age of 1 month ($P < .0001$) (Table 4). The surface moisture content on the forehead, cheek, and forearm was significantly higher than that on the chest on postnatal days 2 to 4 and at the age of 1 month. The moisture content in the stratum corneum was significantly higher on the cheek than on the forehead, chest, or forearm on postnatal days 2 to 4 ($P < .0001$) and was significantly higher on the forearm than on the forehead, cheek, or chest at the age of 1 month ($P < .0001$).

No significant differences in the moisture content of the surface or in the stratum corneum were evident on postnatal days 2 to 4 between infants with and without subsequent AD. In contrast, the moisture content of the surface and stratum corneum of the forehead and cheek at 1 month of age was significantly greater for infants with AD than for those without AD. Infants who developed infantile eczema showed no difference from those who did not in surface or stratum corneum moisture content for any region or time point, except for greater moisture content on the surface of the cheek at the age of 1 month.

Multivariate logistic regression analysis was used to assess independent effects of the various postnatal and prenatal risk factors on development of AD (Table 5). All factors that approached significance with Pearson χ^2 tests, Student's t tests, or Mann-Whitney U tests were included in the model, that is, paternal hay fever, maternal eczema, MIP-1 β levels, surface moisture content on the forehead and cheek, and moisture content of the stratum corneum of the forehead and cheek, all at the age of 1 month. Paternal hay fever (OR: 0.129; 95% CI: 0.020–0.845), MIP-1 β levels (OR: 0.982; 95% CI: 0.967–0.998), and moisture content on the surface of

Family History for AD and Infantile Eczema

	AD			Infantile Eczema		
	Yes (N = 27), n (%)	No (N = 186), n (%)	P	Yes (N = 26), n (%)	No (N = 187), n (%)	P
Paternal history						
Eczema	2 (7.4)	10 (5.4)	.669	2 (7.7)	10 (5.3)	.627
Asthma	1 (3.7)	8 (4.3)	.885	2 (7.7)	7 (3.7)	.348
Hay fever	2 (7.4)	61 (32.8)	.007	8 (30.8)	55 (29.4)	.887
Maternal history						
Eczema	4 (14.8)	8 (4.3)	.027	3 (11.5)	9 (4.8)	.163
Asthma	1 (3.7)	9 (4.8)	.794	1 (3.8)	9 (4.8)	.827
Hay fever	6 (22.2)	49 (26.3)	.647	6 (23.1)	49 (26.2)	.733

Cytokines and Chemokines in Cord Blood According to Development of AD During the First Year and Infantile Eczema During the First Month

	Concentration, Median (interquartile Range), pg/ml					
	AD			Infantile Eczema		
	Yes	No	P	Yes	No	P
IL-2	0.10 (0.10-0.65)	0.10 (0.10-0.10)	.7005	0.10 (0.10-1.50)	0.10 (0.10-0.10)	.6092
IL-6	4.19 (2.18-10.45)	5.67 (1.80-13.34)	.6149	7.86 (3.52-16.40)	5.35 (1.64-12.42)	.1106
IL-8	32.4 (3.3-312.2)	34.5 (4.0-253.1)	.8321	69.5 (9.6-1020.7)	31.6 (3.2-246.5)	.1316
IL-10	0.10 (0.10-0.19)	0.10 (0.10-0.53)	.1939	0.10 (0.10-0.49)	0.10 (0.10-0.48)	.834
GM-CSF	0.10 (0.10-4.02)	0.10 (0.10-6.60)	.2826	2.47 (0.10-19.01)	0.10 (0.10-4.88)	.1719
IFN- γ	0.10 (0.10-0.78)	0.10 (0.10-0.83)	.8562	0.10 (0.10-0.77)	0.10 (0.10-0.83)	.9786
TNF- α	0.18 (0.10-0.65)	0.18 (0.10-0.74)	.7769	0.33 (0.10-0.79)	0.18 (0.10-0.66)	.4371
IL-1 β	0.39 (0.10-1.78)	0.23 (0.10-2.07)	.8969	0.91 (0.10-2.34)	0.15 (0.10-2.00)	.3643
IL-5	0.10 (0.10-0.13)	0.10 (0.10-0.21)	.2485	0.13 (0.1-0.43)	0.10 (0.10-0.17)	.0277
IL-7	0.83 (0.51-1.19)	1.02 (0.64-1.97)	.0783	1.33 (0.68-2.72)	0.96 (0.59-1.65)	.1675
IL-12	0.10 (0.10-0.10)	0.10 (0.10-0.10)	.6068	0.10 (0.10-0.10)	0.10 (0.10-0.10)	.9702
IL-13	0.10 (0.10-0.13)	0.10 (0.10-0.17)	.9104	0.10 (0.10-0.20)	0.10 (0.10-0.17)	.8855
IL-17	0.10 (0.10-1.25)	0.10 (0.10-1.95)	.1791	0.99 (0.10-2.87)	0.10 (0.10-1.36)	.0347
G-CSF	2.53 (8.72-5.86)	2.60 (0.10-8.16)	.7584	4.06 (0.81-13.29)	2.52 (0.10-5.78)	.3418
MCP-1	12.6 (9.0-22.8)	19.4 (10.4-72.9)	.0628	54.8 (17.0-85.6)	16.1 (9.8-63.1)	.0362
MIP-1 β	57.3 (32.0-78.7)	64.0 (42.2-161.6)	.0233	110 (43-287)	62 (39-123)	.1422

GM-CSF indicates granulocyte/macrophage colony-stimulating factor; G-CSF, granulocyte colony-stimulating factor.

Skin Parameters at 2 Days After Delivery and at 1 Month, According to Development of AD During the First Year and Infantile Eczema During the First Month

	AD			Infantile Eczema		
	Yes	No	P	Yes	No	P
Surface moisture, mean \pm SD, μ S						
Forehead						
2 d	0.47 \pm 0.49	0.43 \pm 0.50	.7165	0.43 \pm 0.40	0.44 \pm 0.51	.9196
1 mo	1.88 \pm 0.97	1.44 \pm 0.53	.0016	1.68 \pm 0.78	1.46 \pm 0.57	.0931
Cheek						
2 d	0.58 \pm 0.49	0.49 \pm 0.28	.1728	0.39 \pm 0.17	0.51 \pm 0.52	.0697
1 mo	1.72 \pm 0.86	1.24 \pm 0.43	<.0001	1.63 \pm 0.78	1.24 \pm 0.45	.0004
Chest						
2 d	0.30 \pm 0.21	0.32 \pm 0.25	.7064	0.30 \pm 0.17	0.32 \pm 0.25	.6789
1 mo	1.07 \pm 0.31	1.02 \pm 0.30	.4604	1.03 \pm 0.27	1.03 \pm 0.30	.9609
Forearm						
2 d	0.57 \pm 0.56	0.61 \pm 0.62	.7641	0.69 \pm 0.64	0.59 \pm 0.60	.4786
1 mo	1.54 \pm 0.60	1.40 \pm 0.50	.2532	1.41 \pm 0.44	1.42 \pm 0.44	.9674
Stratum corneum moisture, mean \pm SD, μ S						
Forehead						
2 d	13.5 \pm 3.6	14.2 \pm 5.8	.5435	14.2 \pm 3.8	14.1 \pm 5.8	.9681
1 mo	36.2 \pm 9.0	32.5 \pm 7.8	.0461	34.2 \pm 9.5	32.7 \pm 7.8	.3939
Cheek						
2 d	18.3 \pm 4.9	17.0 \pm 6.1	.3068	16.3 \pm 4.3	17.3 \pm 6.2	.457
1 mo	35.6 \pm 6.5	31.3 \pm 7.1	.0080	32.6 \pm 5.8	31.7 \pm 7.3	.5526
Chest						
2 d	13.9 \pm 2.7	13.8 \pm 3.1	.8630	14.2 \pm 3.0	13.8 \pm 3.0	.5289
1 mo	29.9 \pm 7.2	28.3 \pm 5.7	.2208	27.8 \pm 5.9	28.6 \pm 5.9	.5467
Forearm						
2 d	13.8 \pm 5.9	14.7 \pm 3.4	.5385	16.4 \pm 7.5	14.3 \pm 6.1	.1188
1 mo	45.2 \pm 11.4	41.3 \pm 9.4	.0852	43.4 \pm 9.9	41.5 \pm 9.6	.3705

the cheek at an age of 1 month (OR: 3.189; 95% CI: 1.279-7.952), but no other factors, were significant predictors of AD in the best-fitting model.

DISCUSSION

Development of atopic diseases is thought to depend on a complex interplay of genetic factors, environmental

Multivariate Logistic Regression Results Concerning AD During the First Year of Life

	OR (95% CI)	P
Paternal hay fever	0.129 (0.020-0.845)	.0327
Maternal eczema	2.363 (0.45-12.55)	.3127
MIP-1 β level	0.982 (0.967-0.998)	.0261
Surface moisture		
Forehead, 1 mo	2.118 (0.917-4.892)	.0787
Cheek, 1 mo	3.189 (1.279-7.952)	.0128
Stratum corneum moisture		
Forehead, 1 mo	0.99 (0.914-1.073)	.8107
Cheek, 1 mo	1.039 (0.958-1.126)	.3534

exposure to allergens, and nonspecific adjuvant factors. Only a few prospective birth cohort studies have addressed AD occurring in the first year of life.^{6,7} We found several perinatal predictors of increased risk, including certain physiologic skin parameters, low cytokine concentrations in cord blood, and family history of atopic diseases.

We determined the cumulative incidence of maternally reported, physician-diagnosed AD in the cohort of infants studied to be 27 cases (12.4%) among 213 children, in essential agreement with other epidemiologic studies in the United Kingdom¹² and the German Multicenter Atopy Study,¹³ which showed that 14% and 13.4% of subjects, respectively, developed AD in the first year of life. Our study demonstrated increased risk of AD for infants born to mothers with a history of eczema, which is consistent with previous reports that a positive maternal history predicted greater risk for childhood eczema than did a positive paternal history.¹⁴ Atopy may be inherited preferentially through the maternal line or mothers may carry relatively more of the predisposing genes. Interestingly, we found a negative relationship between AD and paternal history of hay fever caused by Japanese cedar pollen. Genetic susceptibility to hay fever apparently does not contribute to the development of AD in children; indeed, paternal hay fever might provide a child with some protection against developing AD. Kurzius-Spencer et al⁷ similarly found evidence of an apparent protective effect of paternal asthma, but mechanisms underlying these protective effects remain unknown.

Environmental influences during pregnancy and early life, particularly those related to hygiene and infections, seem to increase risks of asthma and allergic disease. In fact, certain infectious complications during pregnancy, such as respiratory tract infections, have shown associations with the development of asthma in childhood.^{15,16} However, we could not detect associations between maternal viral or bacterial infections and the development of AD in children. This disagreement might involve differences in prenatal and postnatal actions of risk factors between various allergic diseases. For example, Calvani et al¹⁷ demonstrated that most such factors

affected mainly the risk of nonatopic but not atopic asthma. Another possible explanation is that our study was prospective, whereas most others had a cross-sectional design.

In the present study, cord blood concentrations of IL-6, IL-8, IL-10, granulocyte/macrophage colony-stimulating factor, TNF- α , IL-1 β , IL-7, IL-17, granulocyte colony-stimulating factor, MCP-1, and MIP-1 β were measurable in >40% of samples. However, other cytokines rarely were present in detectable amounts. The reason for the small number of samples with detectable concentrations of these cytokines might be related to suboptimal methods used for their quantification, because assays for some of the cytokines are known to be technically difficult. Alternatively, it is possible that various immune functions, including the capacity to secrete some cytokines, are attenuated at birth.^{5,18} We could perform no additional analyses of IL-4 because the proportion of samples with detectable concentrations was only 1%.

In the present study, we found negative relationships between cord blood concentrations of MIP-1 β and the risk of AD during the first year of life. We know of no previous reports suggesting that MIP-1 β within the fetoplacental unit might influence susceptibility to subsequent disease development. The ability of chemokines to regulate Th1 and Th2 responses suggests that these mediators may take part in the pathogenesis of atopic diseases such as allergic asthma, for which Th2 response dominance has been observed. Influences of MIP-1 α , MIP-1 β , and regulated on activation, normal T cell expressed and secreted in the establishment of Th1 responses have been reported.¹⁹ Grob et al²⁰ demonstrated intracellular expression of MIP-1 β in CD4⁺ and CD8⁺ T cells from patients with allergic asthma to be significantly less than that in cells from subjects without asthma. This observation of diminished MIP-1 β production by both CD4⁺ and CD8⁺ T cells suggests the relevance of this chemokine to disease development, with relative deficiency being likely to reflect dominance of Th2 responses over Th1 responses at the chemokine level. This view was supported by our present findings showing that low concentrations of cord blood MIP-1 β were related to the risk of AD during the first year of life.

Infants with AD showed a trend toward lower concentrations of IL-7 and MCP-1, although the trend did not reach significance. Schonland et al²¹ demonstrated IL-7 to be a powerful stimulator of neonatal T cells, driving most CD4⁺ and CD8⁺ T cells into the cell cycle. Furthermore, the combinations of IL-4 and IL-12 with IL-7 were found to provide superior enhancement of antigen-specific T cell proliferation.²² Although MCP-1 was originally described for its chemotactic activity on monocytes, *in vitro* studies revealed an even higher activity on T cells.²³ Low concentrations of IL-7 and MCP-1 at birth may lead to impairment of T cell activa-

tion; therefore, infants may develop AD later during the first year of life. Another possible explanation for the lower cytokine levels might be secondary phenomena attributable to a different pattern of specific cell subtypes within the blood of these children. Additional studies are needed to confirm whether infants with AD have significantly lower concentrations of IL-7 and MCP-1 at birth.

In 1997, the European Group for Efficacy Measurements on Cosmetics and Other Topical Products gave recommendations regarding electrical measurement methods.²⁴ According to those recommendations, both single-frequency and multifrequency instruments may be used to assess skin hydration. High-frequency measurements in general reflect the deeper living layers of the skin, whereas low-frequency measurements are dominated by the stratum corneum. In the present study, we used a novel moisture meter (ASA-M1) that measures electrical admittance and susceptance at different excitatory frequencies.¹⁰ We found significant differences between functional skin variables in neonatal life and infancy at the age of 1 month, as well as differences between regions for both neonates and infants. This suggests that stratum corneum function was still adapting to extrauterine life during the period studied. A similar conclusion was drawn when skin surface capacitance and electrical conductance were examined in newborns.²⁵ Hoeger and Enzmann²⁶ found a significant increase in stratum corneum hydration, paralleled by a decrease in skin roughness, in serial measurements at 3 days, 4 weeks, and 12 weeks of age.

To our knowledge, no studies have monitored skin function parameters prospectively, to compare directly children with and without subsequent development of AD. In the present study, we found no differences in the moisture content of the surface or stratum corneum, measured a few days after delivery, between infants with and without development of atopy. In contrast, we found significant differences in the moisture content of the surface and stratum corneum on the face at the age of 1 month. Only 6 of 27 infants who developed AD during their first year had facial infantile eczema at 1 month. Although the other 21 infants had no eczema on the face, certain differences in skin function parameters were demonstrated at 1 month between infants with and without subsequent AD. These data suggest that differences in skin physiologic features between infants with and without AD emerge during the first month of life but not in the first few days. We do not know the mechanisms underlying changes in skin function parameters in infants with AD during the first month of life, but abnormalities during this period may be related to impairment of skin adaptation to extrauterine life.

Dry skin, leading to skin barrier disruption, has attracted attention as a nonallergic etiologic factor in AD.⁹ Several studies have demonstrated lower water-holding

capacity in visually "uninvolved" skin of children with AD, compared with children without AD.⁸ Contrary to our expectation, infants with AD had more moisture content in the surface and stratum corneum at the age of 1 month than did infants without AD. The earliest lesions of infantile AD are erythematous weepy patches on the cheeks, with subsequent extension to the rest of the face and neck. With increasing age, there is a tendency toward drying and thickening of the skin in the involved areas. Therefore, our findings at the age of 1 month may be consistent with the earliest lesions in the clinical course of infantile AD. Furthermore, Yosipovitch et al.²⁸ found a positive relationship between stratum corneum hydration, as evaluated with capacitance measurements, and transepidermal water loss (which reflects skin barrier function in newborns), which indicates that electrical properties of newborn skin may provide an indirect measurement of transepidermal water loss; this was also suggested by Saijo and Tagami²⁷ and Okah et al.²⁸ It will be necessary to monitor the skin physiologic features of these infants during the first year, to understand when the findings may eventually change into dry skin, leading to the defective skin barrier that is known in AD.

Infants with infantile eczema at the age of 1 month showed differences in immunologic and skin physiologic parameters, compared with findings for infants with later development of AD during the first year of life. In fact, infants with infantile eczema showed significantly higher concentrations of IL-5, IL-17, and MCP-1. These data suggest that the intrauterine environment is more likely to reflect the development of infantile eczema, rather than that of AD. Recent data indicate that the proinflammatory cytokine IL-17 stimulates the recruitment and activation of neutrophils and macrophages.²⁹ Furthermore, IL-17 regulates expression of adhesion molecules and chemokines in keratinocytes, which participate actively in skin inflammatory diseases.³⁰ MCP-1 has been shown to induce the migration of monocytes, which form a significant component of the inflammatory reaction taking place in the skin. Accordingly, higher concentrations of IL-17 and MCP-1 in cord blood of infants who later develop infantile eczema at the age of 1 month may contribute to the enhancement of inflammatory reactions in the skin of these infants. Infants who developed infantile eczema showed no difference from those who did not in stratum corneum moisture content for any region or time point, whereas a significant difference was seen for infants who developed AD during their first year. The reason for the difference in skin physiologic parameters for infants with eczema at the age of 1 month and infants with later development of AD during the first year of life remains unknown. However, measurements of skin physiologic parameters seem to be useful to distinguish infants with later devel-

opment of AD from those with infantile eczema at the age of 1 month.

CONCLUSIONS

Our findings indicated that development of AD in infancy may be related to a decrease in MIP-1 β production at birth, greater skin moisture in the surface of the cheek at 1 month of age, and paternal hay fever, in multivariate logistic regression analysis. The majority of risk factors had different effects on infant eczema and AD, which indicates different causes. The number of samples investigated in the present study might be small; larger prospective studies would serve to confirm our results and to explain the possible mechanism of how these factors act.

ACKNOWLEDGMENTS

This work was supported in part by health sciences research grants for research on eye and ear sciences, immunology, allergy, and organ transplantation from the Ministry of Health, Labor, and Welfare of Japan.

We thank Tomoko Endo and Chihiro Ijima for their technical assistance.

REFERENCES

- Charman CR, Williams HC. Epidemiology. In: Bieber T, Leung DYM, eds. *Atopic Dermatitis*. New York, NY: Marcel Dekker; 2002:21-42
- Bergmann RL, Edenharter G, Bergmann KE, et al. Atopic dermatitis in early infancy predicts allergic airway disease at 5 years. *Clin Exp Allergy*. 1998;28:965-970
- Wright AL. The epidemiology of the atopic child: who is at risk for what? *J Allergy Clin Immunol*. 2004;113(suppl):S2-S7
- Tang ML, Kemp AS, Thorburn J, Hill DJ. Reduced interferon- γ secretion in neonates and subsequent atopy. *Lancet*. 1994;344:983-985
- Macaubas C, de Klerk NH, Holt BJ, et al. Association between antenatal cytokine production and the development of atopy and asthma at age 6 years. *Lancet*. 2003;362:1192-1197
- Moore MM, Rifas-Shiman SL, Rich-Edwards JW, et al. Perinatal predictors of atopic dermatitis occurring in the first six months of life. *Pediatrics*. 2004;113:468-474
- Kurzios-Spencer M, Halonen M, Carla Lohman I, Martinez FD, Wright AL. Prenatal factors associated with the development of eczema in the first year of life. *Pediatr Allergy Immunol*. 2005;16:19-26
- Kusunoki T, Asai K, Harazaki M, Korematsu S, Hosoi S. Month of birth and prevalence of atopic dermatitis in school children: dry skin in early infancy as a possible etiologic factor. *J Allergy Clin Immunol*. 1999;103:1148-1152
- Imokawa G, Abe A, Jin K, Higaki Y, Kawashima M, Hidano A. Decreased level of ceramides in stratum corneum of atopic dermatitis: an etiologic factor in atopic dry skin? *J Invest Dermatol*. 1991;96:523-526
- Horikoshi T, Matsumoto M, Usuki A, et al. Effects of glycolic acid on desquamation-regulating proteinases in human stratum corneum. *Exp Dermatol*. 2005;14:34-40
- Jager W, Velthuis H, Prakken BJ, Kuis W, Rijkers GT. Simultaneous detection of 15 human cytokines in a single sample of stimulated peripheral blood mononuclear cells. *Clin Diagn Lab Immunol*. 2003;10:133-139
- Harris JM, Cullinan P, Williams HC, et al. Environmental associations with eczema in early life. *Br J Dermatol*. 2001;144:795-802
- Illi S, von Mutius E, Lau S, et al. The natural course of atopic dermatitis from birth to age 7 years and the association with asthma. *J Allergy Clin Immunol*. 2004;113:925-931
- Liu CA, Wang CL, Chuang H, Ou CY, Hsu TY, Yang KD. Prenatal prediction of infant atopy by maternal but not paternal total IgE levels. *J Allergy Clin Immunol*. 2003;112:899-904
- Hughes H, Jones RCM, De Wright DE, Dobbs FF. Retrospective study of the relationship between childhood asthma and respiratory infection during gestation. *Clin Exp Allergy*. 1999;29:1378-1381
- Copenhaver CC, Gern JE, Li Z, et al. Cytokine response patterns, exposure to viruses, and respiratory infections in the first year of life. *Am J Respir Crit Care Med*. 2004;170:175-180
- Calvani M, Alessandri C, Sopo SM, et al. Infectious and uterus related complications during pregnancy and development of atopic and nonatopic asthma in children. *Allergy*. 2004;59:99-106
- Neaville WA, Tisler C, Bhattacharya A, et al. Developmental cytokine response profiles and the clinical and immunologic expression of atopy during the first year of life. *J Allergy Clin Immunol*. 2003;112:740-746
- Schrum S, Probst P, Fleischer B, Zipfel PF. Synthesis of the CC-chemokines MIP-1 α , MIP-1 β , and RANTES is associated with a type 1 immune response. *J Immunol*. 1996;157:3598-3604
- Grob M, Schmid-Grendelmeier F, Joller-Jemelka HI, et al. Altered intracellular expression of the chemokines MIP-1 α , MIP-1 β , and IL-8 by peripheral blood CD4 $^{+}$ and CD8 $^{+}$ T cells in mild allergic asthma. *Allergy*. 2003;58:239-245
- Schonland SO, Zimmer JK, Lopez-Benitez CM, et al. Homeostatic control of T-cell generation in neonates. *Blood*. 2003;102:1428-1434
- Rustemeyer T, von Blomberg BM, van Hoogstraten IMW, Bruynzeelw DP, Scheper RJ. Analysis of effector and regulatory immune reactivity to nickel. *Clin Exp Allergy*. 2004;34:1458-1466
- Taub DD, Proost F, Murphy WJ, et al. Monocyte chemoattractant protein (MCP)-1, -2, and -3 are chemotactic for human T lymphocytes. *J Clin Invest*. 1995;95:1370-1376
- Berardesca E. EEMCO guidance for the assessment of stratum corneum hydration: electrical methods. *Skin Res Technol*. 1997;3:126-132
- Yosipovitch G, Maayan-Metzger A, Merlob P, Sirota L. Skin barrier properties in different body areas in neonates. *Pediatrics*. 2000;106:105-108
- Hoeger PH, Enzmann CC. Skin physiology of the neonate and young infant: a prospective study of functional skin parameters during early infancy. *Pediatr Dermatol*. 2002;19:256-262
- Saijo S, Tagami H. Dry skin of newborn infants: functional analysis of the stratum corneum. *Pediatr Dermatol*. 1991;8:155-159
- Okah F, Wickert R, Pickens WL, Hoath S. Surface electrical capacitance as a noninvasive bedside measure of epidermal barrier maturation in the newborn infant. *Pediatrics*. 1993;96:688-692
- Sergejeva S, Ivanov S, Lötval J, Lindén A. Interleukin-17 as a recruitment and survival factor for airway macrophages in allergic airway inflammation. *Am J Respir Cell Mol Biol*. 2005;33:248-253
- Albanesi C, Scarponi C, Cavani A, Federici M, Nasorri F, Girolomoni G. Interleukin-17 is produced by both Th1 and Th2 lymphocytes, and modulates interferon- γ - and interleukin-4-induced activation of human keratinocytes. *J Invest Dermatol*. 2000;115:81-87

Determination of structure and transcriptional regulation of *CYSLTR1* and an association study with asthma and rhinitis

Zhang J, Migita O, Koga M, Shibasaki M, Arinami T, Noguchi E.
Determination of structure and transcriptional regulation of *CYSLTR1*
and an association study with asthma and rhinitis.
Pediatr Allergy Immunol 2006; 17: 242–249. © 2005 Blackwell Munksgaard

Pharmacologic studies have revealed that cysteinyl leukotrienes (CYSLTs) act through two receptors, cysteinyl leukotriene receptor 1 (CYSLTR1) and CYSLTR2. CYSLTR1 antagonists are widely used to treat asthma and rhinitis. In this study, we characterized the genomic structure and transcriptional regulation of *CYSLTR1* and examined associations between *CYSLTR1* polymorphisms and asthma/rhinitis. The experiment of rapid amplification of cDNA end revealed that *CYSLTR1* contains three exons and that the entire open reading frame is located in exon 3. Reverse transcriptase-polymerase chain reaction showed that there were multiple splice variants of *CYSLTR1* and that the transcript expression patterns differed from tissues and cell types. The promoter region of *CYSLTR1* is from –665 to –30 bp relative to the transcription start site. We identified four polymorphisms (c.-618-434T/C, c.-618-275C/A, c.-618-136G/A, and 927C/T), and transmission disequilibrium tests revealed that none of these polymorphisms was associated with the development of asthma/rhinitis. However, the TCG and CAA haplotypes in the promoter region caused different transcriptional activity. Our findings indicate that *CYSLTR1* polymorphisms are not likely to be involved in the development of asthma/rhinitis, but it is possible that these polymorphisms could influence drug responses in individuals with atopic diseases.

Jian Zhang¹, Ohsuke Migita¹, Minori Koga¹, Masanao Shibasaki², Tadao Arinami¹ and Emiko Noguchi¹

¹Department of Medical Genetics, Majors of Medical Sciences, Graduate School of Comprehensive Human Sciences, University of Tsukuba, Tsukuba City, Japan,

²Department of Health Science, Tsukuba Technical University, Tsukuba City, Japan

Key words: asthma; cysteinyl leukotriene receptor 1; 5' rapid amplification of cDNA end; splicing variance; polymorphism

Emiko Noguchi, Department of Medical Genetics, Majors of Medical Sciences, Graduate School of Comprehensive Human Sciences, University of Tsukuba, Laboratory of Advanced Research D, 1-1-1 Tennodai, Tsukuba, Ibaraki 305-8577, Japan
Tel.: +81 298 533 352
Fax: +81 298 533 333
E-mail: enoguchi@md.tsukuba.ac.jp

Accepted 4 October 2005

Asthma and allergic rhinitis are considered chronic inflammatory diseases characterized by infiltration of inflammatory cells such as T cells, eosinophils and mast cells (1, 2). Among chemical mediators known to be involved in the pathophysiology of bronchial asthma and rhinitis, cysteinyl leukotrienes (CYSLTs) are considered to be some of the most important mediators because they cause bronchoconstriction, vascular hyperpermeability, and mucous hypersecretion (3, 4). CYSLTs act through cell surface receptors. Pharmacologic studies have revealed that CYSLTs activate at least two receptors, cysteinyl leukotriene receptor 1 (CYSLTR1) and CYSLTR2 (5–7). These receptors have different potencies and affinities for endogenous agonists and different selectivities for antagonists (8, 9). In 1999, the *CYSLTR1* was cloned by ligand fishing

for orphan 7-transmembrane (7TM) receptors (10, 11). The cDNA encodes a protein of 337 amino acids and maps to human chromosome Xq21.1. Northern blotting revealed that *CYSLTR1* is expressed in spleen, peripheral blood leukocytes, lung, pancreas, small intestine, and prostate (10, 11). *In situ* hybridization experiments showed that *CYSLTR1* is present in human lung smooth muscle and lung macrophages (12). In intracellular calcium mobilization assays, CYSLTs increased Ca^{2+} concentrations with a rank order of potency of leukotriene D₄ (LTD₄) > LTC₄ > LTE₄ (10, 11, 13). CYSLTR1 antagonists, such as montelukast (singular), zafirlukast (accolate) and pranlukast (onon), have been widely used to treat asthma. CYSLTR1 antagonists have also proven effective for treatment of allergic rhinitis (14). Equilibrium

and kinetic binding studies yielded a rank order of potency for CYSLTR1 of zafirlukast = montelukast > pranlukast (15).

Studies have indicated that polymorphisms in genes encoding proteins of the leukotriene synthetic pathway contribute to intra-patient variations in clinical responses to CYSLTR1 antagonists. CYSLTs are synthesized through the 5-lipoxygenase (5-LO, *ALOX5*) pathway of arachidonic acid metabolism. *ALOX5* is the first committed enzyme in the biosynthetic pathway leading to production of the leukotrienes (16). *ALOX5* gene promoter polymorphism has been shown to be associated with altered responses to treatment with antileukotriene drugs (17, 18) and airway hyper-responsiveness to methacholine (19). Another member of the pathway, LTC4 synthase (*LTC4S*), is a terminal enzyme that catalyzes the conjugation of unstable LTA4 with reduced glutathione to form LTC4. The -444A/C polymorphism in *LTC4S* is predictive of the clinical response to pranlukast in a Japanese population (20).

These findings suggest that *CYSLTR1* may be a good candidate gene for asthma and allergic rhinitis. A recent screen of the NCBI database (<http://www.ncbi.nlm.nih.gov>) revealed that *CYSLTR1* contains three exons, but the genomic structure and regulatory region of *CYSLTR1* have not been fully characterized. To date, there has been only one study to examine possible associations of allergic diseases with *CYSLTR1* polymorphisms. 927C/T polymorphism in *CYSLTR1* was examined with asthma in 585 Japanese asthmatic patients and 323 controls, but no association was observed (21). In the present study, we characterized the genomic structure of human *CYSLTR1* and performed association studies of asthma/allergic rhinitis with *CYSLTR1* polymorphisms in a Japanese population.

Methods

Subjects

Probands of asthmatic families were mite-sensitive asthmatic children who visited the Pediatric Allergy Clinic of the University Hospital of Tsukuba. A full verbal and written explanation of the study was given to all family members interviewed, and 137 families (466 members), including 45 families used for our previous genome-wide screening (22), gave informed consent and participated in this study. Criteria used for the diagnosis of asthma were as described previously (22).

Probands of the allergic rhinitis families were children with allergic rhinitis who were recruited from three elementary schools and a junior high school in Matsukawa, a farming community in central Japan where orchard grass pollens are thought to be a major cause of seasonal allergic rhinitis. Children with allergic rhinitis were identified through a questionnaire, and diagnosis was made by physicians. Other family members were contacted, and a total of 48 families (188 individuals) who gave informed consent participated in this study. Criteria used for the diagnosis of seasonal allergic rhinitis were as described previously (23). This study was approved by the Committee of Ethics of the University of Tsukuba.

Mutation screening and genotyping

All exons and exon-intron junctions and the 5' flanking region of *CYSLTR1* were amplified by polymerase chain reaction (PCR) from genomic DNAs of 24 unrelated Japanese females with seasonal allergic rhinitis. Genotyping was carried out with the Big Dye Terminator Cycle Sequencing Ready Reaction Kit (Applied Biosystems, Foster City, CA, USA) on an ABI 3100 autosampler (Applied Biosystems).

5' rapid amplification of cDNA end

We carried out 5' rapid amplification of cDNA end (5' RACE) experiments using commercially available RACE-ready human leukocyte and spleen cDNAs (Marathon Ready cDNA; BD Biosciences/Clontech, Palo Alto, CA, USA) according to the manufacturer's instructions. Primers used for the amplification were: 5'-GCCATTGCCAAAGAAGCCTACAACAG-3' and 5'-CCATCCTAATACGACTCACTATAGGGC-3' (AP1) for the first round PCR, and 5'-TGCCTCTTTCTGGCACTGGAGTACCTT-3' and 5'-ACTCACTATAGGGCTCGAGCGGC-3' (AP2) for the nested PCR. The amplified RACE product was cloned in pCR2.1 TOPO-TA cloning vector (Invitrogen, San Diego, CA, USA). Each white (positive) clone was isolated and grown in Luria-Bertani medium with ampicillin overnight. Plasmids were purified by column chromatography (Invisorb Spin Plasmid Mini Kit; Invitex GmbH, Berlin, Germany) and subjected to direct sequencing with M13 primers.

Expression of *CYSLTR1* in tissues

Human multiple tissue, human immune system, and human blood fraction cDNA panels

Table 1. Sequence of primers used in reverse transcriptase-polymerase chain (RT-PCR) reaction and plasmid constructs

RT-PCR	
Primer pair I-III	
Forward	5'-AGAGAAGACTCGTCCCTGCT-3'
Reverse	5'-CTTGATTGCGGAAGTCATCA-3'
Primer pair II-III	
Forward	5'-AGCGTGGGCTTCCTTAATA-3'
Reverse	5'-CTTGATTGCGGAAGTCATCA-3'
Plasmid constructs	
24 bp	
Forward	5'-ATTATAAGCTTAAGCAGGGACGAGTGTCTCTCTT-3'
Reverse	5'-ATTATAGATCTAAGAGAGAAGACTCGTCCCTGCTT-3'
-30 bp	
Forward	5'-ATTATAAGCTTAAGCAGGGACGAGTGTCTCTCTT CAGCTTAGTTCTC-3'
Reverse	5'-ATTATAGATCTCACAGTCACAGAAATCACAGAG AACTAAGCTGAAG-3'
-108 bp	
Forward	5'-ATTATAAGCTTAAGCAGGGACGAGTGTCTCTC-3'
Reverse	5'-AATTATAGATCTTCAAGTTTCACATAATGCCAGTT-3'
-345 bp	
Reverse	5'-AATTATAGATCTTCCAAACACAGGACCATTGA-3'
-665 bp	
Reverse	5'-AATTATAGATCTGGCTACTGCTGGGCTCATATT-3'
-1253 bp	
Reverse	5'-AATTATAGATCTTGTGTGCTGGGGTATGGTA-3'
-1604 bp	
Reverse	5'-AATTATAGATCTAGGGGAGGTAGCAGAGCAA-3'

The forward primer for the constructs of -345 bp, -665 bp, -1253 bp and -1604 bp is the same as that of -108 bp.

(Clontech) were used to analyze expression of *CYSLTRI* in various tissues. PCR primers are listed in Table 1. Resting CD14⁺ (monocytes), CD4⁺ (T helper/inducer cells), CD8⁺ (T suppressor/cytotoxic cells) and CD19⁺ (B lymphocytes) cells were positively selected from mononuclear cells produced by healthy donors by immunomagnetic separation with Dynabeads M-450 (Dyna, Oslo, Norway). Cells were activated with pokeweed mitogen (PWM; Invitrogen) and concanavalin A (ConA; ICN, Costa Mesa, CA, USA) by standard methods, and the degree of activation of lymphocytes was estimated on the basis of morphological criteria (blast morphology and mitoses) and expression of two activation markers, CD25 (interleukin-2 receptor) and CD71 (transferrin receptor). We used glycerol-3-phosphate dehydrogenase (G3PDH) as an internal control for PCR. Amplification conditions were an initial denaturation step at 94°C for 10 min followed by 40, 34 and 30 cycles of denaturation at 94°C for 30 s, annealing at 60°C for 30 s and extension at 72°C for 30 s for primer pairs I-III, II-III and G3PDH, respectively.

RNA preparation and reverse transcriptase-PCR analysis

Lymphocytes from peripheral blood were isolated by Ficoll-Paque gradient centrifugation

(Amersham Biosciences, Piscataway, NJ, USA). Total RNA was isolated from lymphocytes with RNeasy® MiNi Kit (Qiagen, San Diego, MD, USA) and cDNA was prepared with Taqman reverse transcription (RT) reagents (Applied Biosystems) at 25°C for 10 min, 48°C for 30 min, and 95°C for 5 min. Amplification condition consisted of an initial denaturing step of 95°C for 10 min, followed by 38 cycles of 94°C for 30 s, 60°C for 30 s, 72°C for 30 s, with a final incubation at 72°C for 3 min. PCR products were separated by electrophoresis on 15% polyacrylamide gel at 4°C overnight. Bands were excised from the gels and purified with QIA® II Gel Extraction Kit (Qiagen). PCR products were then cloned in pCR2.1 TOPO-TA cloning vector (Invitrogen). Direct sequencing was carried out with the Big Dye Terminator Cycle Sequencing Ready Reaction Kit (Applied Biosystems) on an ABI 3100 autosequencer (Applied Biosystems).

Plasmid construction and transfection, and luciferase assay

Genomic fragments of the 5' flanking region of exon 1 of *CYSLTRI* were amplified with the primers listed in Table 1. PCR products were digested with *Bgl*III and *Hind*III overnight at 37°C and then subcloned in pGL3-Basic vector (Promega, Madison, WI, USA) digested with *Bgl*III and *Hind*III. U937 cells (Cell Resource Center for Biomedical Research, Tohoku University, Miyagi, Japan) were resuspended in RPMI 1640 (Sigma-Aldrich Co., St Louis, MO, USA) supplemented with 10% fetal calf serum (Sigma-Aldrich). Approximately 1×10^7 cells were cotransfected with 30 µg of test construct and 150 ng of pRL-TK (Promega) by electroporation with a Gene Pulsar II (Bio-Rad, Hercules, CA, USA) set at 350 V and 950 µF for U937. Transfected cells were harvested 5 h after transfection. Cells were lysed by the addition of 200 µl of lysis buffer (Promega). A volume of 20 µl of each lysate was used for the luciferase assay with the Dual-Luciferase Reporter Assay System (Promega). The firefly luciferase values were normalized to the Renilla luciferase values of pRL-TK, which were determined at the same time. Reporter activity is presented as the mean of at least three independent measurements.

Statistical analysis

Transmission disequilibrium test (TDT)-chromosome X was analyzed with the UNPHASED package (<http://www.litbio.org/access.htm>) (24). Differences in transcriptional activity in reporter assays were analyzed with the Wilcoxon test.

Results

Isolation of 5' full-length *CYSLTR1* transcripts and structure of the human *CYSLTR1* gene

Current information in the NCBI database (<http://www.ncbi.nlm.nih.gov>) indicates that *CYSLTR1* is composed of three exons and two introns, and the cDNA is 1537 bp long (NM_006639). Our present 5' RACE experiments with cDNAs derived from human leukocytes and spleen were successful and added an additional 225 bp of sequence to the 5' side of the available sequence (Fig. 1a, b). No additional novel exons were detected.

Tissue expression of *CYSLTR1*

Splice variants of *CYSLTR1* were examined with cDNA derived from lymphocytes. Five splice variants were detected, and the structure of each variant is shown in Fig. 2. Variants A and C were the dominant transcripts in lymphocytes. Variant

A was the longest transcript, whereas variant C lacked a part of exon 1. Variant B lacked all of exon 2, and both variant D and variant E lacked a part of exon 1 and all of exon 2. Expression of *CYSLTR1* in various human tissues was analyzed with a PCR-based method (Fig. 3a-c). We designed primers to amplify the regions between exons 1 and 3 (expected product size 691 bp, primer pair I-III) and between exons 2 and 3 (expected product size 189 bp, primer pair II-III) (Fig. 1a). Transcripts including exons 2 and 3 were observed in most tissues analyzed. We observed multiple splice variants in the transcripts including exons 1, 2 and 3. Variant A was the major product in lung, and several splice variants were observed in brain, placenta, liver, kidney and pancreas (Fig. 3a). Variants A and C were observed in tonsil, leukocytes, spleen and lymph node. Variant C was expressed weakly in thymus and bone marrow (Fig. 3b). Variant A was present in resting CD4+, CD14+, CD8+ and CD19+ cells, and in activated CD4+ cells

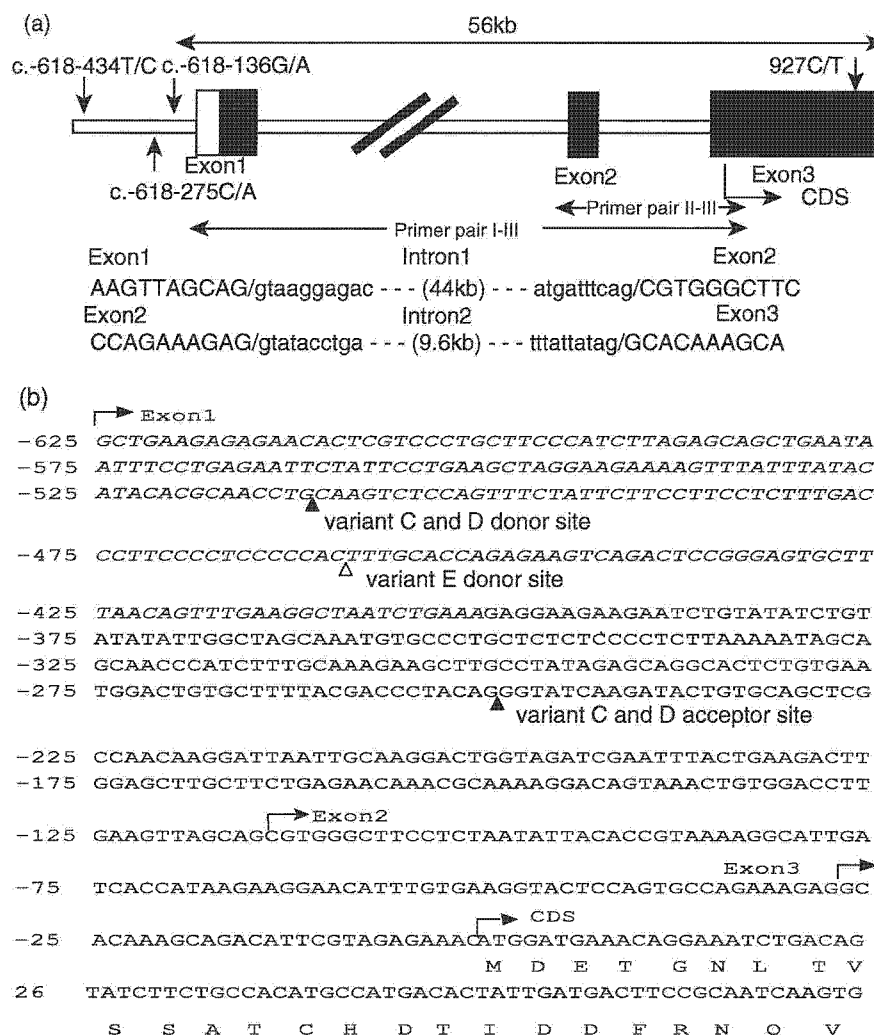


Fig. 1. Genomic structure and cDNA sequence of human cysteinyl leukotriene receptor 1 (*CYSLTR1*). (a) Top, genomic structure of human *CYSLTR1* gene. Boxes mark the positions of exons 1-3. The open box is the region we extended in our 5' rapid amplification of cDNA end (5' RACE) experiment. *CYSLTR1* contains three exons, and the coding sequence (CDS) starts with exon 3. Arrows indicate the locations of the polymorphisms. The positions of primer pairs I-III and II-III are shown. Bottom, genomic sequences of exon-intron junctions in *CYSLTR1*. (b) Sequence of the human *CYSLTR1* cDNA. Numbers are relative to the translation initiation site. Boundaries between exons are indicated by arrows. The 5' RACE extended sequence is italicized. Splice sites for variants C and D are indicated with closed triangles, and the splice site for variant E is shown with an open triangle.

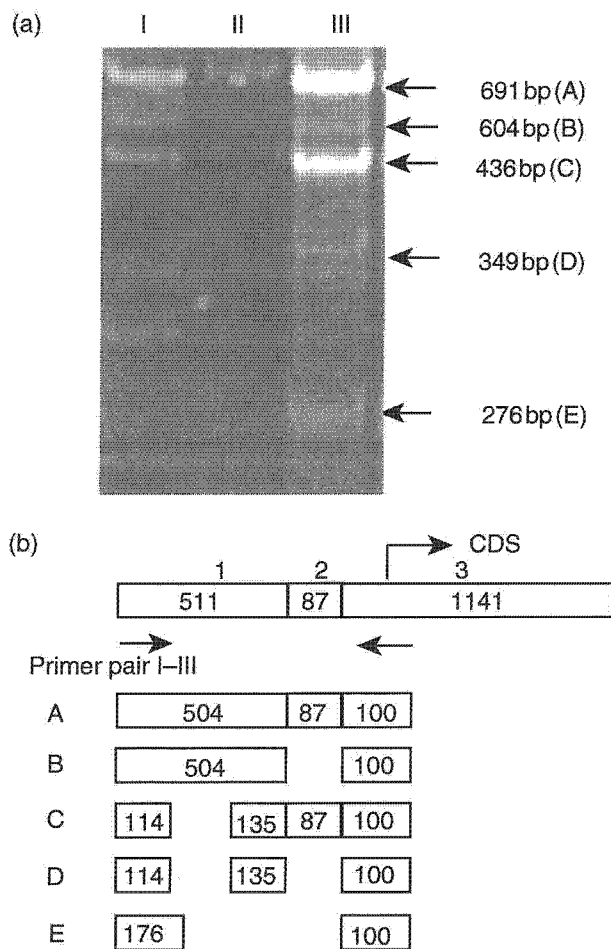


Fig. 2. Splice variants of cysteinyl leukotriene receptor 1 (*CYSLTR1*). There are five *CYSLTR1* variants in lymphocytes (a) and the structure of each variant is shown in (b). The size in bp of each exon is indicated in the box. CDS and arrows indicate the start site of the coding sequence.

and monocytes, but was not expressed in activated CD8+ cells (Fig. 3c). We could not find a human sequence corresponding to band X, which was observed in kidney, fetal liver, tonsil and leukocytes (Fig. 3a, b), by BLAST search with human genome sequence database (<http://www.ncbi.nlm.nih.gov/BLAST/>), therefore, we considered band X as PCR artifact.

Polymorphism search and TDT analysis

We screened for polymorphisms in DNAs from 32 unrelated female subjects and found four polymorphisms c.-618-334T/C (rs321029), c.-618-275C/A (rs2637204), c.-618-136G/A (rs2806489) and 927C/T (rs20995), in *CYSLTR1* (Fig. 1a). We numbered these according to the recommendation of nomenclature system published previously (25). These four polymorphisms are in

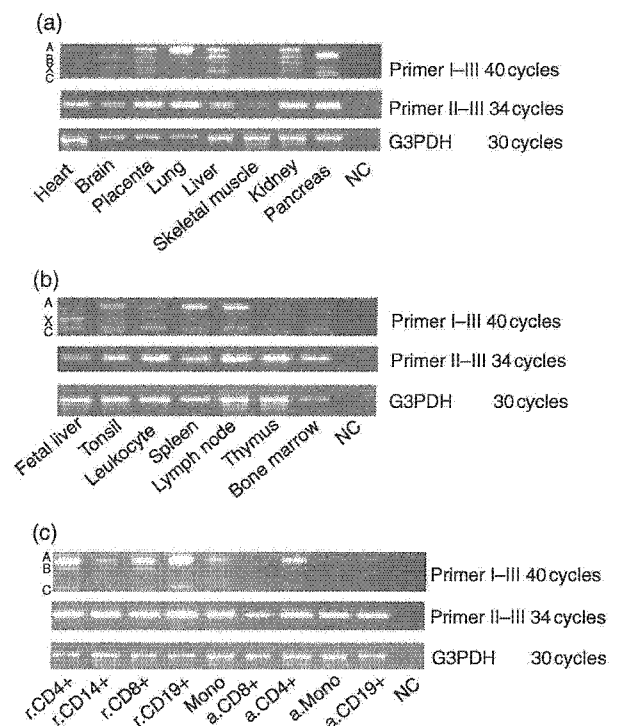


Fig. 3. Expression of cysteinyl leukotriene receptor 1 (*CYSLTR1*) in human multiple tissue panels. Results of polymerase chain reaction amplification of body organs (a), immune system (b), and blood fractions (c) are shown. Glycerol-3-phosphate dehydrogenase is included as an internal control. Mono, monocytes; r, resting; a, activated; NC, no-template control. Four bands (A, B, X and C) were observed, and the splice structures of bands A, B and C are depicted in Fig. 2b.

complete linkage disequilibrium with each other ($r^2 = 1$). We performed TDT analysis of chromosome X, and none of the polymorphisms was associated with asthma or allergic rhinitis (CAAT haplotype: transmitted 26, not transmitted 26, $p = 1.0$ for asthma; and transmitted 12, not transmitted 10, $p = 0.67$ for rhinitis). The frequency of CAAT haplotype in parents was 56% and that of the TCGC haplotype was 44%.

Transcriptional activities of 5' flanking region of *CYSLTR1*

To examine the transcriptional activity in the 5' flanking region of *CYSLTR1*, we constructed plasmids that contained sequences from -1604, -1235, -665, -345, -108, and -30 to +24 relative to the transcription initiation site. The primers used for plasmid construction are listed in Table 1. The expression of *CYSLTR1* in U937 cells was confirmed by RT-PCR (data not shown). These constructs were then transiently transfected into U937 cells. Deletion analysis revealed that the region driving maximal reporter

gene expression in U937 cells was located -665 bp proximal to the transcription initiation site (Fig. 4). Two larger constructs, one from -1604 and the other from -1235, have lower luciferase activities than construct -665, suggesting that negative regulatory sites may be present in this region.

To determine whether the c.-618-434T/C, c.-618-275C/A, and c.-618-136G/A polymorphisms are functional, we generated luciferase reporter gene constructs that contained the 5' flanking region of *CYSLTR1* from exon 1 to -665 bp, and differed from wildtype only with c.-618-434C, c.-618-275A, and c.-618-136A. The three polymorphisms in the promoter (c.-618-434T/C, c.-618-275C/A, and c.-618-136G/A) and 927C/T are in complete linkage disequilibrium ($r^2 = 1$) with each other, so only two promoter haplotypes (TCG and CAA) exist in the population. The construct containing the TCG haplotype had higher transcriptional activity than that containing the CAA haplotype ($p = 0.049$), suggesting that the TCG and CAA haplotypes have different transcriptional activities and may contribute to altered expression of *CYSLTR1* (Fig. 5).

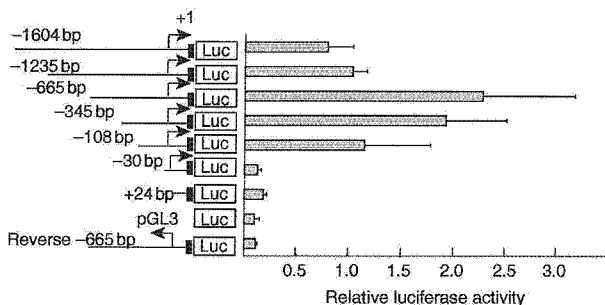


Fig. 4. Reporter activity in U937 cells. Each construct was transfected into U937 cell as described in *Methods*. Luciferase activity is presented relative to Renilla activity, and all values are the mean \pm s.d. of at least three independent experiments.

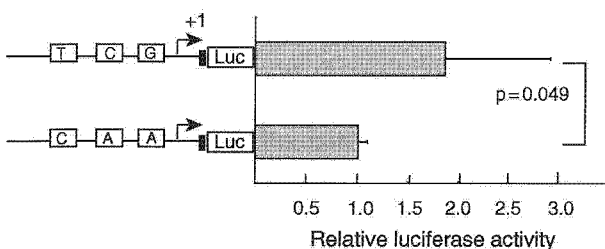


Fig. 5. Effect of the three polymorphisms on cysteinyl leukotriene receptor 1 (*CYSLTR1*) promoter activity. Luciferase activity is presented relative to Renilla activity, and values are the mean \pm s.d. of at least three independent experiments.

Discussion

In the present study, we investigated the genomic structure and transcriptional activity of *CYSLTR1* and examined possible associations of *CYSLTR1* polymorphisms with asthma/rhinitis. We isolated the full-length genomic region of *CYSLTR1* and characterized the promoter region of *CYSLTR1*. We found four polymorphisms in *CYSLTR1*, but none was associated with asthma or allergic rhinitis by TDT.

Our 5' RACE analysis revealed that *CYSLTR1* contains three exons and extended the previous sequence data by 225 bp on the 5' side. Exons 1 and 2 are non-coding, and the entire open reading frame is located in exon 3. We found that there are five different *CYSLTR1* transcripts in lymphocytes. These transcripts do not change the putative open reading frame; all variants are predicted to encode identical proteins. However, it is possible that the differences in the transcripts influence the stability or secondary structure of the mRNA, which alters translation of the transcript to protein.

Genome-wide analyses of alternative splicing indicate that 40–60% of human genes have alternative splice forms, suggesting that alternative splicing is one of the most significant components of the functional complexity of the human genome (26). Recent studies showed that a majority of alternative splices change the protein product (26, 27). However, in the present study, the alternative splicing sites in the variants occurred outside of the coding region. This suggests that a strict conformation of the *CYSLTR1* protein is essential for its function in leukotriene signaling.

Tissue distribution of *CYSLTR1* has been examined extensively. Northern blot analysis revealed the highest level of expression in peripheral blood leukocytes, followed by spleen, lung, pancreas, small intestine and other tissues (10, 11). RT-PCR and *in situ* hybridization showed expression in eosinophils, neutrophils, B cells, T cells, mast cells, and CD14+, CD19+ and CD34+ cells (12, 28, 29). In the present study, we examined expression of the different transcripts in many tissues. Transcripts including exons 2 and 3 were observed in most tissues tested. However, expression of transcripts originating from exon 1 varied significantly in different tissues. Our data suggest that transcripts originating from exon 1 are the dominant transcripts in some tissues, such as thymus and bone marrow. Interestingly, transcripts from exon 1 were observed in resting CD8+ cells but not in activated CD8+ cells, suggesting that expression

- human lung parenchyma. *Biochem Pharmacol* 2002; 63: 1537–46.
16. SAMUELSSON B, DAHLEN SE, LINDGREN JA, ROUZER CA, SERHAN CN. Leukotrienes and lipoxins: structures, biosynthesis, and biological effects. *Science* 1987; 237: 1171–6.
 17. IN KH, ASANO K, BEIER D, et al. Naturally occurring mutations in the human 5-lipoxygenase gene promoter that modify transcription factor binding and reporter gene transcription. *J Clin Invest* 1997; 99: 1130–7.
 18. DRAZEN JM, ISRAEL E, O'BYRNE PM. Treatment of asthma with drugs modifying the leukotriene pathway. *N Engl J Med* 1999; 340: 197–206.
 19. KIM SH, BAE JS, SUH CH, NAHM DH, HOLLOWAY JW, PARK HS. Polymorphism of tandem repeat in promoter of 5-lipoxygenase in ASA-intolerant asthma: a positive association with airway hyperresponsiveness. *Allergy* 2005; 60: 760–5.
 20. ASANO K, SHIOMI T, HASEGAWA N, et al. Leukotriene C4 synthase gene A(–444)C polymorphism and clinical response to a CYS-LT(1) antagonist, pranlukast, in Japanese patients with moderate asthma. *Pharmacogenetics* 2002; 12: 565–70.
 21. UNOKI M, FURUTA S, ONOUCHI Y, et al. Association studies of 33 single nucleotide polymorphisms (SNPs) in 29 candidate genes for bronchial asthma: positive association a T924C polymorphism in the thromboxane A2 receptor gene. *Hum Genet* 2000; 106: 440–6.
 22. YOKOUCHI Y, NUKAGA Y, SHIBASAKI M, et al. Significant evidence for linkage of mite-sensitive childhood asthma to chromosome 5q31-q33 near the interleukin 12 B locus by a genome-wide search in Japanese families. *Genomics* 2000; 66: 152–60.
 23. YOKOUCHI Y, SHIBASAKI M, NOGUCHI E, et al. A genome-wide linkage analysis of orchard grass-sensitive childhood seasonal allergic rhinitis in Japanese families. *Genes Immun* 2002; 3: 9–13.
 24. DUDBRIDGE F, KOELEMAN BP, TODD JA, CLAYTON DG. Unbiased application of the transmission/disequilibrium test to multilocus haplotypes. *Am J Hum Genet* 2000; 66: 2009–12. E-pub Apr 13.
 25. ANTONARAKIS SE. Recommendations for a nomenclature system for human gene mutations. Nomenclature Working Group. *Hum Mutat* 1998; 11: 1–3.
 26. MODREK B, LEE C. A genomic view of alternative splicing. *Nat Genet* 2002; 30: 13–9.
 27. KAN Z, ROUCHKA EC, GISH WR, STATES DJ. Gene structure prediction and alternative splicing analysis using genomically aligned ESTs. *Genome Res* 2001; 11: 889–900.
 28. MELLOR EA, MAEKAWA A, AUSTEN KF, BOYCE JA. Cysteinyl leukotriene receptor 1 is also a pyrimidinergic receptor and is expressed by human mast cells. *Proc Natl Acad Sci U S A* 2001; 98: 7964–9.
 29. MITA H, HASEGAWA M, SAITO H, AKIYAMA K. Levels of cysteinyl leukotriene receptor mRNA in human peripheral leucocytes: significantly higher expression of cysteinyl leukotriene receptor 2 mRNA in eosinophils. *Clin Exp Allergy* 2001; 31: 1714–23.



Gene expression profiling defined pathways correlated with fibroblast cell proliferation induced by *Opisthorchis viverrini* excretory/secretory product

Chanitra Thuwajit, Peti Thuwajit, Kazuhiko Uchida, Daoyot Daorueang, Sasithorn Kaewkes, Sopit Wongkham, Masanao Miwa

Chanitra Thuwajit, Peti Thuwajit, Daoyot Daorueang, Sopit Wongkham, Department of Biochemistry, Liver Fluke and Cholangiocarcinoma Research Center, Faculty of Medicine, Khon Kaen University, Khon Kaen 40002, Thailand

Sasithorn Kaewkes, Department of Parasitology, Liver Fluke and Cholangiocarcinoma Research Center, Faculty of Medicine, Khon Kaen University, Khon Kaen 40002, Thailand

Kazuhiko Uchida, Masanao Miwa, Institute of Basic Medical Science, University of Tsukuba, Tsukuba, Ibaraki 305-8575, Japan

Supported by the Thailand Research Fund, Grant No. TRG4880004 and the Grants of Khon Kaen University 2004 and 2006; Grants-in-Aid for Scientific Research from the Ministry of Education, Science, Sports and Culture of Japan; the Grant for Student of Liver Fluke and Cholangiocarcinoma Research Center, Faculty of Medicine, Khon Kaen University, 2003-2005

Co-first authors: Peti Thuwajit

Correspondence to: Chanitra Thuwajit, PhD, MD, Department of Biochemistry, Faculty of Medicine, Khon Kaen University, Khon Kaen 40002, Thailand. tchani@kku.ac.th

Telephone: +66-43-348386 Fax: +66-43-348386

Received: 2006-02-01 Accepted: 2006-03-01

transduction, protein synthesis and translation, matrix and structural protein, transcription control, cell cycle and DNA replication. Moreover, the expressions of serine-threonine kinase receptor, receptor tyrosine kinase and collagen production-related genes were up-regulated by *O. viverrini* ES product. The expression level of signal transduction genes; *pkC*, *pdgfra*, *jak 1*, *eps 8*, *tgfb 1i4*, *strap* and *h ras* measured by real-time RT-PCR confirmed their expression levels to those obtained from cDNA array. However, only the up-regulated expression of *pkC*, *eps 8* and *tgfb 1i4* which are the downstream signaling molecules of either epidermal growth factor (EGF) or transforming growth factor- β (TGF- β) showed statistical significance ($P < 0.05$).

CONCLUSION: *O. viverrini* ES product stimulates the significant changes of gene expression in several functional categories and these mainly include transcripts related to cell proliferation. The TGF- β and EGF signal transduction pathways are indicated as the possible pathways of *O. viverrini*-driven cell proliferation.

© 2006 The WJG Press. All rights reserved.

Key words: Gene expression profile; *Opisthorchis viverrini*; Excretory/secretory product; cDNA array; Fibroblast; Cell proliferation; Signal transduction; Cholangiocarcinogenesis

Thuwajit C, Thuwajit P, Uchida K, Daorueang D, Kaewkes S, Wongkham S, Miwa M. Gene expression profiling defined pathways correlated with fibroblast cell proliferation induced by *Opisthorchis viverrini* excretory/secretory product. *World J Gastroenterol* 2006; 12(22): 3585-3592

<http://www.wjgnet.com/1007-9327/12/3585.asp>

Abstract

AIM: To investigate the mechanism of fibroblast cell proliferation stimulated by the *Opisthorchis viverrini* excretory/secretory (ES) product.

METHODS: NIH-3T3, mouse fibroblast cells were treated with *O. viverrini* ES product by non-contact co-cultured with the adult parasites. Total RNA from NIH-3T3 treated and untreated with *O. viverrini* was extracted, reverse transcribed and hybridized with the mouse 15K complementary DNA (cDNA) array. The result was analyzed by ArrayVision version 5 and GeneSpring version 5 softwares. After normalization, the ratios of gene expression of parasite treated to untreated NIH-3T3 cells of 2-and more-fold upregulated was defined as the differentially expressed genes. The expression levels of the signal transduction genes were validated by semi-quantitative SYBR-based real-time RT-PCR.

RESULTS: Among a total of 15 000 genes/ESTs, 239 genes with established cell proliferation-related function were 2 fold-and more-up-regulated by *O. viverrini* ES product compared to those in cells without exposure to the parasitic product. These genes were classified into groups including energy and metabolism, signal

INTRODUCTION

An *Opisthorchis viverrini* infection or opisthorchiasis is the most important health problem in Southern Asia, including Northeastern Thailand, Laos, Vietnam and southern China^[1]. It is a definite cause of bile duct cancer or cholangiocarcinoma (CC) in humans and has been classified as a carcinogen. Parkin *et al*^[2] performed

a case-control study of patients and estimated that two-thirds of CC cases in Thailand were caused by *O. viverrini* infestation. Nowadays, CC remains a major public health problem in many parts of Southeast Asia. The incidence rate of CC around the world is different with increasing tendency^[3,4]. The highest incidence is in the Northeastern part of Thailand with the rate of 188 per 100 000^[5]. The pathogenesis of *O. viverrini*-associated CC may be a complex process, involving several mechanisms. The effect of parasites on the bile duct epithelium is classified, as both mechanical and chemical irritations. The mechanical irritation is the direct contact of parasites to the bile duct epithelium; the chemical irritation is believed to be caused by the excretory/secretory (ES) product released from the flukes. These chronic irritations caused by the parasite later result in the proliferation of bile duct epithelium and leads to epithelial hyperplasia^[6]. This is an important step in the genesis of cancer because hyperplastic cells are vulnerable to a carcinogen and can easily turn to adenomatous and finally cancerous cells^[7]. Moreover, the alterations of immune response and the stromal cells which are mainly composed of fibroblasts were observed in opisthorchiasis and CC in both animal models and human. The fibrosis and mononuclear cell infiltration with lymphocyte aggregation and, additionally, ductal dilatation were observed in the gall bladders and extrahepatic bile ducts of the hamsters infected with *O. viverrini*^[8]. In addition, the chronic inflammation and fibrosis of the bile ducts may contribute to the strikingly enhanced susceptibility to CC among people with heavy liver fluke infection^[9]. The malignant transformation of bile duct epithelium via dysplasia was detected in the abnormal intrahepatic biliary tree of the patients with congenital hepatic fibrosis^[10]. There is the important relationship between the gradual decreases of inflammation with a concomitant increase in fibrosis after *O. viverrini* re-infection in the experiment hamsters^[11]. All of these data provide evidence of the importance of fibrosis in the formation of cholangiocarcinoma.

Fibrosis is the excessive accumulation of extracellular matrix proteins produced from the active and accumulated fibroblasts. It occurs in most types of chronic diseases including chronic liver disease. Liver fibrosis is considered a model of the wound-healing response of the liver to repeated injury^[12]. Activated hepatic stellate cells, portal fibroblasts, and myofibroblasts have been identified as the major collagen-producing cells in the repeatedly injured liver^[13]. In the fibrogenesis, the increased numbers and then the accumulation of fibrogenic cells including the fibroblasts and myofibroblasts are the main observations. As aforementioned, there is the correlation of fibrosis with the development of CC. The interaction of *O. viverrini* and the host immune cells has been proven to be the main causative issue for chronic inflammation in opisthorchiasis. The cytokines released from the immune cells will lead to the formation of fibrosis later. Moreover, direct contact of *O. viverrini* which have been strongly proven to induce bile duct epithelium erosion and cell proliferation replacement that occurs later on, may indirectly induce the surrounding fibroblasts around the affected area to proliferate^[14]. The importance of hyperproliferative fibroblasts regarding

the induction of epithelial cancer has been increasingly reported^[15,16]. Though this phenomenon has not been investigated in CC, the direct effect of *O. viverrini* ES product to induce fibroblast cell proliferation has recently been reported *in vitro*^[14,17]. So far, there are no data for the explanation of the fibroblast cell proliferation induced by the *O. viverrini* ES product.

From all the evidence described above, it would appear to be of great interest to study the mechanism of how *O. viverrini* ES product induces fibroblast cell proliferation. In order to know the response of cell to *O. viverrini* ES product, the gene expression analysis of fibroblast cell non-contact co-cultured with adult *O. viverrini* was performed. The expression level of genes was compared to those without *O. viverrini* ES product treatment. The cell proliferation-associated gene expression was discussed in relation to their roles in *O. viverrini* ES product-induced fibroblast cell proliferation. The expression levels of some signal transduction genes were also analyzed and validated by real-time RT-PCR to indicate the possible signal transduction pathway(s) utilized by *O. viverrini* in the induction of fibroblast cell proliferation.

MATERIALS AND METHODS

Parasite preparation

Opisthorchis metacercariae were obtained from naturally infected cyprinoid fish captured from fresh-water reservoirs in the endemic area of Khon Kaen province, Thailand. Pepsin-HCl was used to digest the flesh to obtain metacercariae, which were then introduced to the 6-8-wk-old hamsters *ad libitum*. After 1 mo, the adult *O. viverrini* were collected from the bile ducts of the hamsters and were washed several times with PBS containing 100 mg/L penicillin and 100 kU/L streptomycin. To prevent microbial contamination, the adult *O. viverrini* were then incubated for 30 min in PBS containing antibiotics before being used in the non-contact co-culture technique. The animal holding protocol was approved by the Animal Ethics Committee of Khon Kaen University (AEKKU011/04), based on the Ethics of Animal Experimentation of National Research Council of Thailand.

Cell culture and non-contact co-culture

To prepare the fibroblasts stimulated with *O. viverrini* ES product, the non-contact co-culture between the fibroblasts and the adult parasites was performed. The mouse fibroblast cell line, NIH-3T3, was bought from the American Type Culture Collection (ATCC; Manassas, VA, USA). It was maintained in DMEM (Gibco, Gaithersburg, MD, USA) containing 100 mL/L calf serum (CS) (Gibco, Gaithersburg, MD, USA), designated as the complete medium, followed by incubation in a 50 mL/L CO₂ incubator at 37°C and passaging twice a week. Trypan blue staining was used to measure the viability of cells. The cells with more than 95% viability were collected for performing non-contact co-culture.

The NIH-3T3 cells and the intact viable *O. viverrini* were non-contact co-cultured in a 24-well transwell (Costar, Corning Incorporated, Cambridge, NY, USA). The

parasites were incubated in the upper chamber containing the 8- μ m porous plate, which allowed the ES product to diffuse to the lower chamber where the NIH-3T3 cells adhered. The cell proliferation induction of ES product to the NIH-3T3 cells was confirmed by the viable cell count using trypan blue staining. Briefly, 10 000 NIH-3T3 cells were plated onto the lower chamber of a 24-well double-chamber culture plate for 2 d with complete medium to let most of cells adhere to the well. Then the media were changed to DMEM without CS, serum-free medium. Five viable adult *O. viverrini* were added to the upper chamber of each well. The NIH-3T3 cells cultured in complete medium and serum-free medium were used as positive and negative controls, respectively. The cell numbers obtained from the *O. viverrini* treatment cultured for 2 d was compared to those of the negative and positive controls with the same culturing time.

Hybridization and array data analysis

The in-house prepared mouse cDNA array was prepared by Dr. Kazuhiko Uchida, Department of Biochemistry and Molecular Oncology, Comprehensive Human Science, Graduate School, University of Tsukuba, Japan. It consists of 15 K of either mouse or human genes/ESTs. Firstly, the total RNA extraction from NIH-3T3 cells treated and untreated with adult *O. viverrini* ES product was performed. Briefly, total of 2.5×10^6 cells were collected in RNeasy lysis solution (Ambion[®], Hilden, Germany) and processed for total RNA with a commercial kit (ISOGEN; Nippon Gene, Tokyo, Japan) according to the manufacturer's protocol. The RNA quality was confirmed by subjecting the samples to electrophoresis on formaldehyde-agarose gel and staining the 18S and 28S RNA bands for visualization. Then, a 2- μ g portion of the intact total RNA was dissolved in 8 μ L of RNase-free water, and 2 μ L of oligo (dT) primer (1 g/L; Invitrogen, Carlsbad, CA, USA) was then added. The sample was heated for 10 min at 70°C and immediately chilled on ice. The following reagents were then added to the sample: 5 μ L of first-strand cDNA synthesis buffer, 1 μ L of DTT (0.1 mol/L final concentration), 1.5 μ L of deoxynucleotide triphosphates (20 mmol/L dATP, dGTP, and dTTP), 1.5 μ L of SuperScript (200 MU/L; Invitrogen), and [α -³²P]dCTP (111 PBq/mol; Amersham). The reaction was incubated at 37°C for 90 min. Labeled cDNA was then denatured for 3 min at 95°C. The array was prehybridized at 42°C for 2 h in MicroHyb solution (Invitrogen, Carlsbad, CA, USA) with 0.5 mg/L poly(dA) and 1 mg/L *COT1* DNA (Invitrogen, Carlsbad, CA, USA). The probes were hybridized at 42°C overnight in the same solution. The membrane array was washed twice at 50°C with $2 \times$ SSC-10 g/L SDS for 20 min and at room temperature with $0.5 \times$ SSC-10 g/L SDS for 15 min. The membrane array was exposed to an imaging plate which was scanned with a BAS 5000 Imaging Analyzer (Fuji Film, Tokyo, Japan). Spot intensity was quantified with ArrayVision version 5.0 software (Imaging Research, Ontario, Canada). GeneSpring version 5.0 software (Silicon Genetics, Redwood, CA) was used to normalize values for each gene for data analysis.

Real-time RT-PCR

The mRNA was isolated using a Total RNA Extraction Miniprep System (Viogene, Fegersheim, France) according to the manufacturer's instructions. The DNA contaminated in the extracted RNA was destroyed by DNaseI (Promega Corporation, Madison, WI, USA) at 37°C for 30 min. The DNaseI inactivation reaction was performed at 75°C for 10 min. The first-strand cDNA was synthesized from 1 μ g of mRNA using the Reverse Transcription System (Promega Corporation, Madison, WI, USA). Semi-quantitative PCR was performed with the SYBR-based method in 12.5 μ L reaction in Rotor Gene RG-3000 (Corbett Research). After the denaturing of cDNA at 95°C for 10 min, the reaction profile was subjected to 50 amplification cycles, each cycle consisted of denaturation at 95°C for 30 s, annealing at different temperatures for each gene (52, 55, 58, 58, 54, 52, 52, 52, 65, and 60°C for *abl 1*, *pkC*, *pdgfra*, *jak 1*, *eps 8*, *tgfb 14*, *strap*, *csnk 1 α 1*, *b ras*, and *β m*, respectively) for 30 s, and extension at 72°C for 45 s. After the PCR, a melting curve was constructed by increasing the temperature from 50 to 99°C. β 2-microglobulin (β m), whose expression was found to be directly proportional to the amount of mRNA that presented in the sample stimulated by any growth factors^[18], was used as the internal control. The standard curve between the CT of each gene expression and the amount of the starting total RNA was performed. The CT of the samples was then compared to the corresponding standard curve and quantitated the amount of the starting mRNA in that sample. The RT-PCR was performed three times for each gene.

Table 1 shows the PCR primers designed by the Gene Fisher Program according to the mRNA sequences of each gene in the GenBank database. The primer sequences can then be categorized into groups of growth factors they belong to, in this case, the signal transduction molecules. The result was analyzed for the statistical significance by STATA version 8 (StataCorp LP, Texas, USA).

RESULTS

Gene responding to *O. viverrini* ES product

Using a mouse cDNA array, we examined the gene expression profile of cell proliferation stimulated by *O. viverrini* ES product. A total of 15 000 genes and ESTs were tested. *O. viverrini* caused widespread alteration in gene expression. The ratios of gene expression between treated and untreated with the parasite ES product equal and greater than 2 were focused on because of their striking changes. Among all genes/ESTs in 15K cDNA array, 885 genes fitted to this criterion. Among these genes, only 536 genes had a variety of molecular functions and only 239 genes within these 536 genes had cell proliferation-related functions. These 239 genes were categorized in groups as proteins playing roles in energy and metabolism, signal transduction, protein synthesis and translation, matrix and structural protein, transcription control, cell cycle and DNA replication. The percentage distribution of genes in each group is 25.2, 21, 18.9, 17,

Table 1 List of signal transduction genes¹ validated the expression by real-time RT-PCR, their corresponding PCR primers², annealing temperature and product sizes

Group of stimulating Gene	Primer sequence	Annealing temperature (°C)/ product size (bp)
PDGF /EGF	Forward: 5'-TGAAGTTGGTGGGCTGCA-3'	52/148
	Reverse: 5'-TTTTCACCTGGGCCCGCA-3'	
<i>pkC</i>	Forward: 5'-GGCATGCCTTGTCTGGAGA-3'	55/149
	Reverse: 5'-TGTAGCCCTGCCTCGAGAGA-3'	
<i>jak 1</i>	Forward: 5'-CAGCCCTCGCTCGTCTT-3'	58/147
	Reverse: 5'-CCAAGCCCTCAGAGCT-3'	
<i>raf 1</i>	Forward: 5'-TTTCCGGATGCCTGCTA-3'	62/147
	Reverse: 5'-TCCTGCTGCCATGCA-3'	
<i>h ras</i>	Forward: 5'-TGGTGGGCAACAAGTGTA-3'	65/150
	Reverse: 5'-CCGAATTTATGTGCCGAA	
PDGF	Forward: 5'-TGC GGGAAGGACTGGA-3'	58/122
	Reverse: 5'-GTGAGGAGACAGCTGAGGA-3'	
EGF	Forward: 5'-CCGCTCCGTGGTATGGA-3'	54/146
	Reverse: 5'-ACGTCCGACACACTGCTGA-3'	
TGF-β	Forward: 5'-CCAAGTGTGGTAGCTATCGA-3'	52/136
	Reverse: 5'-CAGATTGTTCTCTGCTCC-3'	
<i>strap</i>	Forward: 5'-GCCGGAGATACAGGAGA-3'	52/153
	Reverse: 5'-TGCTTATGAGCCGGTCA-3'	

¹They are classified based on their functions as the downstream signaling molecules of the specific growth factor. ²Primers for the internal control (β -m) are: 5'-CATGGCTCGCTCGGTGA-3' (forward) and 5'-AATGTGAGCGGGTGGAA-3' (reverse). The annealing temperature and the product size of RT-PCR for β m are 60°C and 148 bp, respectively. PDGF: platelet-derived growth factor; EGF: epidermal growth factor; TGF-β: transforming growth factor-β.

12.6, 3.3, and 2, respectively. The examples of genes in each group are summarized in Table 2.

Response of signal transduction-related genes to *O. viverrini* ES product

A total of 59 genes/ESTs categorized by their molecular function as the signal transduction genes showed 2-fold and more up-regulation after *O. viverrini* ES product stimulation. They are the downstream signal transduction molecules for a variety of growth factors. The signal transduction genes that corresponded to the stimulation of either PDGF or EGF, PDGF, EGF and TGF-β were categorized and summarized in Table 3. The most up-regulated expressions were *tgfβ 1i4* and *abl 1* which are the representatives of TGF-β- and either PDGF- or EGF-stimulated signal transduction pathways, respectively.

In addition to the different signal transduction molecules responded to different growth factors, the receptors for PDGF/EGF and TGF-β are classified in different types as tyrosine kinase and serine-threonine kinase receptors, respectively. The cDNA array data represented the different up-regulated expression levels between these 2 types of receptors (Table 4).

Nine signal transduction genes, which responded to the specific growth factor as mentioned in Table 3, were selected and tested for their expression levels by semi-quantitative RT-PCR. The single peak of the melting curve for each gene confirmed the appropriate PCR condition (data not shown). The result indicated similar responses in both cDNA array and RT-PCR analyses of *pkC*, *jak 1*, *b*

ras, *pdgfra*, *eps 8*, *tgfβ 1i4*, and *strap*. However, the significant ($P < 0.05$) up-regulation was only found for those of *pkC*, *eps 8*, and *tgfβ 1i4*. The opposite result of mRNA expression level was detected in *abl 1* and *raf 1* (Figure 1).

DISCUSSION

Cell proliferation is regulated by the intricacy of cell growth regulators, signaling cascades, and mediators of cell cycle progression including cyclins, cyclin-dependent kinases (CDKs). Anti-proliferative genes coding for the apoptotic protein, cyclin/CDK inhibitors are important in controlling cell proliferation. Addition of growth factors induces cell proliferation including the fibroblasts^[19]. The changes in gene expression that accompany this proliferative response have been the subject of many studies, and the responses of dozens of genes have been characterized^[19]. A recent study indicated the effect of *O. viverrini* ES product in induction of fibroblast cell proliferation *in vitro*^[17]. We have examined the effect of this parasitic product in the gene expression profile using a cDNA array. The NIH-3T3 cells were used because it not only had the marked response to *O. viverrini* ES product^[17], but also being classified as the mesenchymal cells as the real target of *O. viverrini* ES product; the stellate cells and myofibroblasts. Among all genes/ESTs in 15K cDNA array, 885 genes showed 2-fold and more up-regulation after stimulation by *O. viverrini* ES product. Among these genes, only 536 genes had a variety of established molecular functions. Moreover, 239 of these 536 genes had cell proliferation-related functions and were primarily focused into groups based on their specific functions because of their striking increased changes (≥ 2 -fold).

Most of the genes which increased their expression by *O. viverrini* ES product stimulation were the proteins controlling the enzymatic metabolism and biosynthesis. The expressions of glyceraldehyde-3-phosphate dehydrogenase, alpha-enolase and aldehyde dehydrogenase involve the glycolysis pathway. Cytochrome C oxidase and ATP synthase involve energy production from the electron transport chain. These phenomena could be easily understood because high levels of energy production and synthesis of biological macromolecules are required for the stimulation of quiescent fibroblasts by *O. viverrini* ES product into the cell cycle progression. These data suggest the possibility that ES product acts like a growth factor to stimulate cell proliferation basically by the stimulation of energy production-related gene expression^[20].

In cell proliferation, the DNA replication is needed. Many proteins, including RPII215 polymerase and topoisomerase II, required for chromosome segregation at mitosis; and DNA primase, required for DNA replication, all increased their expressions in *O. viverrini* ES product-treated cells. These increased expressions will help cells undergo into cell cycle and consequently cell division. Ribonucleotide reductase is associated with the anabolic pathway of deoxynucleotide. The increased expression of this enzyme causes an increase in the deoxynucleotide triphosphate (dNTP) pool in the nucleus, which facilitates DNA synthesis and repair^[21]. In addition, when cells are activated by the growth factors and then commit to enter

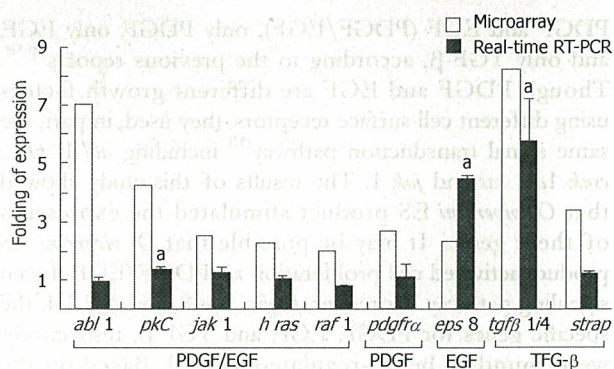


Figure 1 RT-PCR analysis of signal transduction genes up-regulation by *O. viverrini* ES product. The results of DNA array and RT-PCR are shown in comparison for each gene (mean \pm SD, $^{\circ}$ $P < 0.05$).

Table 2 Proliferation-related genes with 2-fold and more¹ up-regulation in fibroblast cell proliferation activated by *O. viverrini* ES product compared to the negative control (not exhaustive)

A Energy and metabolism	Glyceraldehyde-3-phosphate dehydrogenase (<i>gapd</i>), cytochrome C oxidase, alpha-enolase, ATP synthase beta subunit ² , thioredoxin, aldehyde dehydrogenase
B Signal transduction	Transforming growth factor beta-1-induced transcript 4 (<i>tgfb 1i4</i>), tyrosine kinase (<i>abl 1</i>), interleukin 1 receptor-associated kinase, MAP kinase phosphatase (<i>mkp 6</i>), colony stimulating factor 3 receptor, protein kinase C, Janus kinase 2 (<i>jak 2</i>), casein kinase I alpha (<i>csnk 1a1</i>), <i>c-myc</i>
C Protein synthesis and translation	Polyubiquitin C (<i>Ubc</i>) gene, ribosomal protein S27a ² , ribosomal protein L27, elongation factor Tu, RNA polymerase 1-2, translation initiation factor 4 gamma ²
D Matrix and structural protein	Lysophospholipase 1 (<i>lypla 1</i>)
E Transcription control	Transformation/transcription domain-associated protein (<i>trrap</i>) ² , telomeric repeat binding factor 1 (<i>terf 1</i>), transcription factor EB (<i>tcfeb</i>), DEAD-box RNA helicase (<i>ddx 21</i>) ²
F Cell cycle	Kinesin family member 3a (<i>kif 3a</i>), mitotic kinesin-linked protein 1 ² , cyclin-dependent kinase 4 (<i>cdk 4</i>), <i>cdk 5</i> , cyclin B1
G DNA replication	RPII215 polymerase II large subunit, topoisomerase II alpha, DNA primase p58 subunit (<i>prim 2</i>), ribonucleotide reductase

¹Sequence in each group is ordered from high to low expression increases; ²represents human gene.

the cell cycle, the cascade of gene expression within the cells is needed. This means it is important that the initial gene expressed to be protein for the expression of the

Table 3 Up-regulation of signal transduction-related genes in NIH-3T3 treated with *O. viverrini*, categorized in groups according to the response to the specific growth factor

Related growth factor (Accession number)	Gene name/production	Folding
PDGF/EGF		
AW544655	Tyrosine kinase (<i>v abl</i>)	7.12
C80388	Protein kinase C (<i>pkc</i>)	4.23
AU042564	Casein kinase I-alpha isoform (<i>csnk 1a 1</i>) ¹	3.81
C87299	Casein kinase I-epsilon (<i>csnk 1e</i>)	2.88
AU046274	Ras-GTPase activating protein SH3-domain binding protein (<i>c3bp</i> -pending)	2.73
C87788	JAK1 protein tyrosine kinase	2.56
AU017366	<i>H ras</i>	2.26
AW552623	<i>N ras</i>	2.01
PDGF		
AW537708	PDGF receptor, alpha-polypeptide (<i>pdgfr a</i>)	2.64
EGF		
C88280	Epidermal growth factor receptor pathway substrate (<i>eps 8</i>)	2.32
TGF-β		
AW546174	Transforming growth factor beta-1-induced transcript 4 (<i>tgfb 1i4</i>)	8.24
AU016757	<i>c myc</i>	3.70
C79202	Serine/threonine kinase receptor-associated protein (<i>strap</i>)	3.40

¹Represents human gene.

Table 4 cDNA array analysis showing up-regulation of genes encoded for the kinase receptors

Receptor kinases	Gene names (accession number)	Folding
Serine-threonine kinase	Serine/threonine kinase 11 (C85710)	4.42
	Serine/threonine kinase 19 (AW557191)	3.28
	Serine/threonine kinase 4 (AU020804)	2.88
Tyrosine kinase	TYRO3 protein tyrosine kinase 3 (AW556118)	2.60
	JAK1 protein tyrosine kinase (C87788)	2.56
	Protein tyrosine kinase 9 (AW544421)	1.83
	Downstream of tyrosine kinase 1 (AW557123)	1.59

later ones. This is the action of protein classified as the transcription factor. In cells treated with *O. viverrini* ES products, a variety of transcription factors are activated.

Cyclins and CDKs are the important proteins in cell cycle progression^[22]. The response of cell to *O. viverrini* ES product indicated the increased expression of many CDKs and cyclins. CDK4 and 5 are important at the G1 phase, whereas cyclin B1 is crucial in G2 phase. The increased expression of phosphorylated cyclin D1 was reported in fibroblast proliferation induced by *O. viverrini* ES product^[17], thereby supporting the increased expression of

CDK4 in this study. This result supports the importance of cyclin D1-CDK4 expression in the re-entry of the serum-stimulated fibroblasts into the cell-division cycle^[23]. Moreover, *O. viverrini* ES product induced the expression of kinesins which are a family of microtubules and are involved in many crucial cellular processes including cell division^[24]. The kinesin family member 3a (*kif 3a*) and mitotic kinesin-like protein are crucial for spindle assembly and function, chromosome segregation, mitotic checkpoint control, and cytokinesis in higher eukaryotes^[25]. Cells cannot divide without the appropriate functions of these genes.

Rapid and efficient production of macromolecule in protein synthesis and degradation of superfluous proteins play important role in cell cycle progression^[26]. The increased RNA polymerase which determines the efficiency of mRNA production supports the capability of other genes to increase their expressions. The ribosomal proteins as the component of ribosomes, translation initiation factors and elongation factors increased their expressions which normally occur to promote proteins synthesized for cell division. In addition, the expression of polyubiquitin C (*ubc*) increased to get rid of the superfluous proteins already synthesized and that have reached their expired period. The increased expression of these genes is crucial for the turnover of the appropriate proteins for the right stimuli at the right time.

Matrix and structural proteins are important in supporting cell proliferation^[27]. In this study, some matrix and structural proteins increased their expression level by *O. viverrini* ES product stimulation. Lysophospholipase D (lysoPLD) catalyses the production of lysophosphatidic acid (LPA) from the lysophosphatidylcholine (LPC). LPA has been demonstrated to be a potent inducer of cell proliferation of multiple cell lineages^[28]. Taken together, all the data presented in this study confirm that *O. viverrini* ES product can activate cell proliferation resulting in the response of gene expression profile like a serum or growth factor^[29].

Array analysis is not only crucial in understanding the effect of the ES product on cells but also to predict what should be the growth factor available in *O. viverrini* ES product. In this work, we took the advantage of this technology to decipher the possible genome expression circuit induced by *O. viverrini* ES product. The comparison of *O. viverrini* ES product-induced gene expression profile with that of established growth factor profiles may be useful to know the cell signaling pathway utilized by *O. viverrini* ES product in induction of cell proliferation. The *O. viverrini* ES product stimulated cell proliferation like the response of cells to the calf serum^[19]. There are many types of growth factors contained in the calf serum including platelet-derived growth factor (PDGF), epidermal growth factor (EGF), transforming growth factor- β , and insulin-like growth factor (IGF). Each of them stimulates a different signal transduction profile which is the most important feature used to distinguish the types of growth factor-stimulated cell responses^[30,31]. In this study, the signal transduction genes selected from the array data can be categorized based on their functions as the downstream signal transduction molecules of both

PDGF and EGF (PDGF/EGF), only PDGF, only EGF, and only TGF- β , according to the previous reports^[30,31]. Though PDGF and EGF are different growth factors using different cell surface receptors, they used, in part, the same signal transduction pathway^[32] including *abl 1*, *pkc*, *csnk 1a1*, *ras* and *jak 1*. The results of this study showed that *O. viverrini* ES product stimulated the expression of these genes. It may be possible that *O. viverrini* ES product activated cell proliferation via PDGF/EGF-driven signaling pathway. Moreover, *pdgfra*, *eps 8*, and *tgfb 1i4*, the specific genes for PDGF, EGF, and TGF- β , respectively, were found to be up-regulated as well. Based on the increased expression, *tgfb 1i4* was ranked in the uppermost expression level. It is supposed that *O. viverrini* ES product stimulated cell proliferation via TGF- β signaling pathway as well.

The difference between signal transduction pathways activated by TGF- β and PDGF/EGF is mainly focused on their different types of receptors. The receptors of TGF- β are membrane-bound receptors exhibiting intrinsic serine-threonine kinase activities, whereas the tyrosine kinase receptor is activated by EGF or PDGF^[30,31]. From cDNA array data, the activation of serine-threonine kinase and tyrosine kinase receptors encoded gene expression showed the involvement of both types of receptors in the stimulation by *O. viverrini* ES product. This evidence still supports the possibility that TGF- β and EGF/PDGF can be the candidate signal transduction pathway induced by *O. viverrini* ES product.

Since the uncertain mRNA expression level was detected by cDNA array analysis, RT-PCR was used to measure the exact expression. From the list of up-regulated signal transduction-related genes, we selected 9 genes for additional analysis to validate the array expression data. The result showed marked increase of *tgfb 1i4* expression. It has been proven that *tgfb 1i4* is a direct target of TGF- β ^[33,34] and also is the transcriptional modulator stimulated by TGF- β . The *tgfb 1i4* gene expression was transcriptionally activated by TGF- β , phorbol 12-myristate 13-acetate, and serum but not appreciably by EGF^[34]. The up-regulation of *tgfb 1i4* expression induced by *O. viverrini* ES products may indicate the stimulation of the TGF- β -activated signal transduction pathway. The normal expression of *strap*, the inhibitor of the TGF- β signal transduction cascade^[35], supports this conclusion.

For the EGF and PDGF-stimulated signal transduction pathways, the expressions of the common genes, including *abl 1*, *jak 1*, *h ras* and *raf 1*, were not significantly increased. Moreover, the specific gene related to PDGF-stimulated signal transduction, *pdgfra*, was expressed at the same level as in cells without *O. viverrini* ES product treatment. This result excludes the potential of *O. viverrini* ES product in stimulating cell proliferation through the PDGF-mediated signal transduction pathway. For the EGF-stimulated signal transduction pathway, *eps 8* is the transcription factor required in the EGF-stimulated cell proliferation and is confirmed to be the gene product that represents a novel substrate for tyrosine kinase receptors^[36]. Adoptive expression of *eps 8* cDNA in fibroblastic or hematopoietic target cells expressing the EGFR resulted in an increased mitogenic response to EGF, implicating the *eps 8* product